

Magnetic field estimates for accreting neutron stars in massive binary systems and models of magnetic field decay

Chashkina, A.^a, Popov, S.B.^b

^a*Sternberg Astronomical Institute, Moscow State University, Moscow, Russia 119992;
Email: sagitta.minor@gmail.com*

^b*Sternberg Astronomical Institute, Moscow State University, Moscow, Russia 119992;
Email: polar@sai.msu.ru*

Abstract

Some modern models of neutron star evolution predict that initially large magnetic fields rapidly decay down to some saturation value $\sim \text{few} \times 10^{13}$ G and weaker magnetic fields do not decay significantly (Pons et al., 2009). It is difficult to check the predictions of this model for initially highly magnetized objects on the time scale of a few million years. We propose to use Be/X-ray binaries for this purpose. We apply several methods to estimate magnetic fields of neutron stars in these accreting systems using the data obtained by the RXTE satellite (Galache et al., 2008). Only using the most modern approach for estimating the magnetic field strengths of long period NSs as proposed by Shakura et al. (2011) we are able to obtain a field distribution compatible with predictions of the theoretical model of field decay of Pons et al. (2009).

Keywords: accretion, accretion discs, star: magnetic fields, binaries

1. Introduction

Neutron stars (NSs) are the final stage of the evolution of massive stars. There are different types of young isolated NSs: radio pulsars (see a review in Manchester et al. 2005), compact central X-ray sources in supernova remnants (Pavlov et al., 2004; de Luca, 2008), magnetars: anomalous x-ray pulsars (AXPs) and soft gamma-ray repeaters (SGRs) (Mereghetti, 2008; Rea and Esposito, 2011), close-by cooling radioquiet isolated NSs – the Magnificent seven (M7) (Haberl, 2007; Kaplan, 2008), rotating radio transients

(RRATs) (Keane, 2010). Another large class of observed systems with NSs is formed by X-ray binaries. They are subdivided into high mass X-ray binaries (HMXB) and low mass X-ray binaries (LMXB) (see a review on X-ray binaries and their evolution in Postnov and Yungelson (2006); Bhattacharyya (2009)).

In order to deeper comprehend the evolution and to follow links between different types of NSs we need a better understanding of the basic processes related to NS thermal and magneto-rotational evolution. For the initially highly magnetized NSs ($B \gtrsim \text{few} \times 10^{13}$ G), modern models predict that the magnetic field decays significantly on the time scale of several hundred thousand years (Aguilera et al., 2008). For magnetars there is a strong observational evidence for magnetic field decay (see, for instance, Pons and Geppert (2007) and references therein). These sources are very young NSs with ages of the order of tens of thousand years or less and with magnetic fields $10^{14} - 10^{15}$ G. Unfortunately, it is difficult to use magnetars for testing models of magnetic field decay on a time scale $\gtrsim 10^6$ yrs because they become extremely elusive and avoid detection at ages more than about a hundred thousand years.

For “standard” values of the initial magnetic fields ($10^{11} - 10^{13}$ G) typical for radio pulsars the field decay in these models is insignificant: the magnetic field diminishes just by a factor of 2. Therefore, the population of radio pulsars is ill-suited to test these model predictions.

Popov et al. (2010) carried out a comprehensive population synthesis of young NSs (radio pulsars, magnetars, near-by cooling NSs) and showed that a model with magnetic field decay can explain the basic properties of all the three populations considered using the same initial magnetic field distribution. All types of these objects have ages less than \sim million years. It is important to find a way to confront model predictions and observations on a longer time scale. NSs in some HMXBs can be suitable for testing the evolution of magnetic fields on the time scales of several million years. Compact objects in these systems have average ages \sim a few million years (their massive companions usually have a total lifetime less than 10-30 million years). In the case of wind-fed accretion (Negueruela, 2010), the accretion rate is not large enough to affect significantly the evolution of the field (as opposed to systems with intense disc accretion which produce millisecond pulsars). Thus, by estimating magnetic fields of NSs in HMXBs with accretion from a wind, it is possible to study the magnetic field evolution on the time scale of a few million years.

The most numerous homogeneous class of HMXBs are Be/X-ray binaries (Liu et al., 2006; Reig, 2011). Now there are about 70 objects of this type known in the Galaxy, 78 in the Small Magellanic Cloud (SMC), and 16 in the Large Magellanic Cloud (Raguzova and Popov, 2005). We consider 40 Be/X-ray binaries in the SMC to estimate magnetic fields of NSs by means of different methods.

The article is structured as follows. In Sec. 2 we describe the model of the magnetic field decay that we compare our estimates with. In Sec. 3 we present different methods to obtain estimates of magnetic fields of accreting NSs. In Sec. 4 we present the observational data used in the paper. Sec. 5 contains our results, and in Sec. 6 we discuss them.

2. Magnetic field decay model

In this section we describe an analytical approximation for the model of field decay used in this paper, following the approach suggested by Aguilera et al. (2008) and discuss types of objects that can be used for testing this model.

There are several mechanisms for the magnetic field decay, but the rate of field decay is mainly determined by the Ohmic decay and the Hall drift. The Ohmic decay involves diffusion of the magnetic field lines with respect to the charged particles. The characteristic Ohmic time scale is (Goldreich and Reisenegger, 1992):

$$\tau_{Ohm} = \frac{4\pi\sigma\lambda^2}{c^2}. \quad (1)$$

Here λ is the typical magnetic field length scale and σ is the conductivity of NS matter, c is the speed of light.

The Hall drift time scale is:

$$\tau_{Hall} = \frac{4\pi en_e\lambda^2}{cB}. \quad (2)$$

Here n_e is electron density and B is magnetic field strength. The Hall drift can transport magnetic field from the inner crust where the Ohmic decay is slow, to the outer crust where it proceeds rapidly. Unlike the Ohmic decay, the Hall drift is essentially a non-linear process.

As we can see, the characteristic time scales of field decay strongly depend on the length scale. This brings us to the problem of magnetic field localization. If the magnetic field is distributed in the entire NS, including the core, then these time scales are long so that the magnetic field decay is insignificant on time scales about few million years. In the modern

models (Aguilera et al., 2008; Pons et al., 2009) it is assumed that the main part of the magnetic field is localized in the crust of a NS. In this case $\tau_{Ohm} \sim 10^5 - 10^6$ yrs and $\tau_{Hall} \sim (10^2 - 10^4)(B_0/10^{15}\text{G})^{-1}$ yrs.

The evolution of magnetic field according to the model by Aguilera et al. (2008); Pons et al. (2009) is well approximated by the following equation:

$$B(t) = B_{\min} + (B_0 - B_{\min}) \frac{\exp(-t/\tau_{Ohm})}{1 + \tau_{Ohm}/\tau_{Hall}(1 - \exp(-t/\tau_{Ohm}))}. \quad (3)$$

Here B_0 is the initial magnetic field strength ¹ and $B_{\min} = \min[B_0/2, 2 \times 10^{13}]$ G. It can be seen that an initially strong magnetic field evolves to the asymptotic value $B = 2 \times 10^{13}$ G, which can be slightly different for different objects. It is probably so in the case of magnetar SGR 0418+5729, which was born with high magnetic field strength and evolved to the value $B < 7.5 \times 10^{12}$ G (Rea and Esposito, 2011). For low-field objects the decay is not so pronounced and the field decays just by a factor of 2. Therefore according to the theory, there should be only a small number of objects with strong magnetic fields among populations of sources with ages $\sim 10^6$ yrs, for example among HMXBs.

It is convenient to illustrate the evolution of the magnetic field on the $P - \dot{P}$ diagram. The results of evolution according to the eq. (3) for different τ_{Ohm} and τ_{Hall} are shown in four panels of Fig.1. In each panel evolutionary tracks are shown for different initial magnetic fields from 10^{12} G to 10^{16} G. The observed populations indicated in the plots are the following: pulsars (black dots), magnetars (open diamonds), five of the M7 (triangles), and RRATs (filled diamonds). According to the simple model of field decay (eq. 3) sooner or later magnetic fields of initially strongly magnetized NSs converge to the asymptotic value $B \sim 2 \times 10^{13}$ G, and clustering of sources can be visible. For PSRs, M7, or any other population this effect is not visible in the data. Therefore we can assume that this convergence should happen at larger ages, where no isolated NSs are observed now.

The plot for a more realistic set of parameters is shown in the top left panel: $\tau_{Ohm} = 10^6$ yrs and $\tau_{Hall} = 10^4(B_0/10^{15}\text{G})^{-1}$ yrs. Therefore, we use these parameters for theoretical estimates in sections 5 and 6. At the other panels the convergence is too rapid to be consistent with the observational picture.

¹Below we discuss the field values at the magnetic pole: $B \equiv B_{pole} = 2B_{equator} = 2\mu/R^3$, where R is the radius of a NS. For numerical estimates we use the value $R = 10^6$ cm.

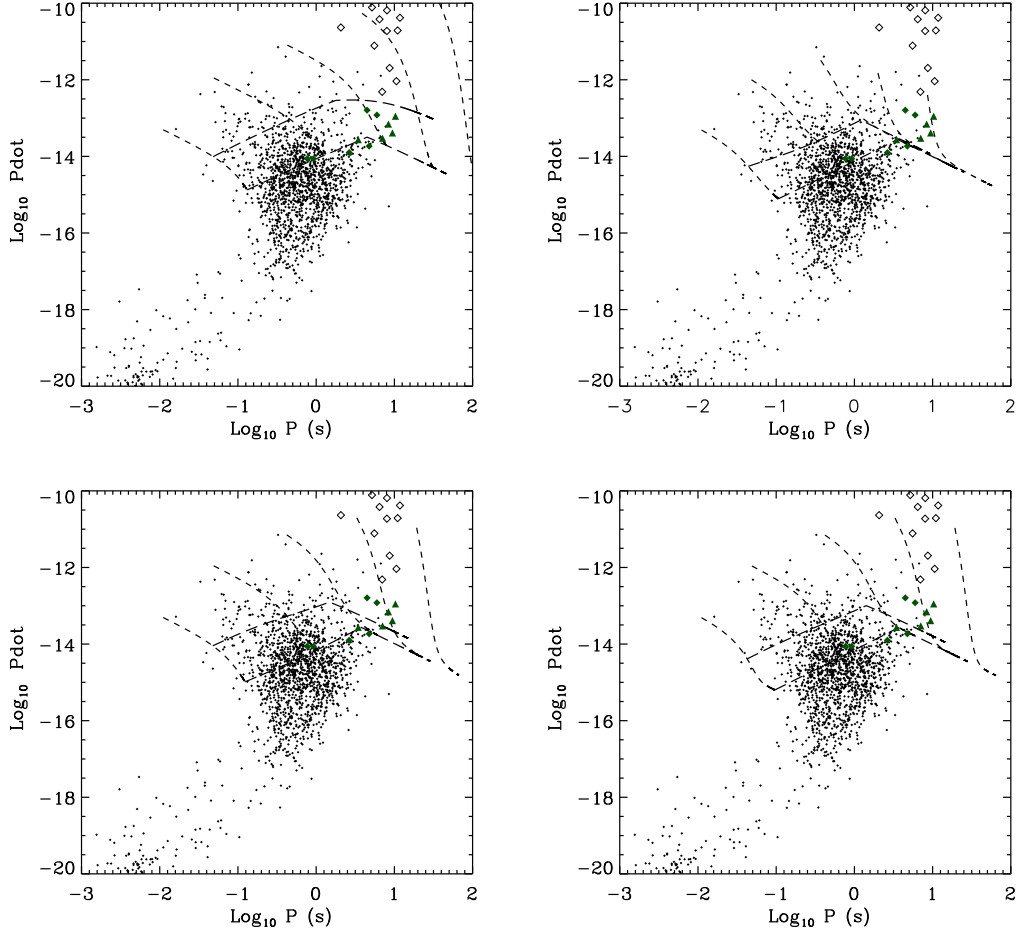


Figure 1: $P - \dot{P}$ diagram of radio pulsars, magnetars and radio-quiet isolated NSs. The observed populations indicated in the plots are the following: pulsars (black dots), magnetars (open diamonds), five of the M7 (triangles), and RRATs (filled diamonds). In each panel NSs evolutionary tracks are shown according to analytical approximation of the field decay model (Eq. 3) with different initial magnetic fields from 10^{12} G to 10^{16} G. In different panels different τ_{Ohm} and τ_{Hall} are used. Top left: $\tau_{Ohm} = 10^6$ yrs, $\tau_{Hall} = 10^4(B_0/10^{15}\text{G})^{-1}$ yrs. Top right: $\tau_{Ohm} = 10^7$ yrs, $\tau_{Hall} = 10^2(B_0/10^{15}\text{G})^{-1}$ yrs. Bottom left: $\tau_{Ohm} = 10^6$ yrs, $\tau_{Hall} = 10^3(B_0/10^{15}\text{G})^{-1}$ yrs. Bottom right: $\tau_{Ohm} = 10^5$ yrs, $\tau_{Hall} = 10^3(B_0/10^{15}\text{G})^{-1}$ yrs. Tracks are plotted for $B_0 = 10^{12}, 10^{13}, 10^{14}, 10^{15}$, and 10^{16} G. In all cases NSs are treated as orthogonal rotators according to the magnetodipole formula. Long-dashed lines correspond to ages 10^5 and 10^6 yrs.

The convergence must occur beyond the death line. Then PSRs cannot be used to test this effect. The M7-like sources are too cold when the convergence appears. Magnetars are not active any more when the field reaches to the asymptotic value. We propose that determination of the magnetic fields of NSs in HMXBs can be used to see the effect of convergence on the time scale of few million years. We use Be/X-ray binaries to test predictions of theoretical models of field decay.

3. Methods of magnetic field evaluation

In this section we describe several methods to estimate the magnetic field of accreting NSs used in this paper. At first, we discuss the equilibrium period hypothesis in the case of wind and disc accretion. Then, we formulate the models based on the values of maximal observed rates of spin-down and spin-up of an accreting NS. After that we present the model based on the assumption of the equality of Alfvén and corotation radii at the moment of appearance of pulsations. Finally, we summarize three more sophisticated models: the model by Illarionov and Kompaneets (1990), the model by Bisnovatyi-Kogan (1991), and a new approach based on the model by Shakura et al. (2011).

3.1. The equilibrium period hypothesis

In an accreting system a NS is affected by accelerating and decelerating torques (see, for instance, Lipunov (1992) to which we refer for details of accretion physics basics). The spin-up of a NS is due to the orbital angular momentum brought by the accreted matter. In the case of disc accretion the accelerating torque can be represented as a flow of angular momentum transported from the last Keplerian orbit:

$$K_{su,disc} = \dot{M} \sqrt{GM\epsilon R_A}. \quad (4)$$

For wind accretion the following equation can be used:

$$K_{su,wind} = \dot{M} \eta \Omega R_G^2. \quad (5)$$

Here \dot{M} is the accretion rate, $R_A = (\mu^2/2\dot{M}\sqrt{GM})^{2/7}$ is the Alfvén radius, M is the NS mass, $\Omega = 2\pi/P_{orb}$ is its orbital frequency, and $R_G = 2GM/(v_{orb}^2 + v_{wind}^2)$ is the Bondi radius, v_{wind} is the stellar wind velocity, v_{orb}

is the orbital velocity, ϵ, η – some numerical coefficients, whose values depend on the properties of the accretion flow.

To determine the Bondi radius, R_G , we use the orbital velocity of a NS at periastron. For the eccentricity we use the value $e = 0.3$ as the typical one for Be/X-ray systems (Reig, 2011). We take the stellar wind velocity $v_{wind} = v_0(r/R_*)^{3/2}$ (Raguzova and Lipunov, 1998), where v_0 is the wind velocity at the surface of a Be-star, r is the radius of a circumstellar outflowing disc, and R_* is the Be-star radius. We use the following values: $v_0 = 10 \text{ km s}^{-1}$, $r/R_* = 10$.

The decelerating torque arises due to the magnetic field interaction with the accretion flow. This torque at the stage of accretion can be estimated as follows (Lipunov, 1992):

$$K_{sd} = -k_t \frac{\mu^2}{R_{co}^3}. \quad (6)$$

Here μ is the magnetic moment of a NS and $R_{co} = (GMP^2/4\pi^2)^{1/3}$ is the corotation radius, P – the spin period of NS. k_t is a numerical coefficient dependent on the model of interaction between the magnetosphere and surrounding matter.

The rate of changes of the total angular momentum of a NS can be written down as follows:

$$\frac{dI\omega}{dt} = \begin{cases} \dot{M}\sqrt{GM\epsilon R_A} - k_t\mu^2/R_{co}^3, & \text{for disc accretion} \\ \dot{M}\eta\Omega R_G^2 - k_t\mu^2/R_{co}^3, & \text{for wind accretion} \end{cases} \quad (7)$$

where $I = 10^{45} \text{ g cm}^2$ is the NS moment of inertia and $\omega = 2\pi/P$ – is the spin frequency.

The equilibrium hypothesis states that an accreting NS spends most of the time in the state with decelerating and accelerating moments nearly equalized. When accretion starts the system rapidly evolves towards the equilibrium state (see also section 5). This state is characterized by a characteristic spin period, P_{eq} . To calculate it we use the following values of numerical coefficients (Lipunov, 1992): $\epsilon = 0.45$, $\eta = 1/4$, $k_t = 1/3$. For the case of disc accretion the equilibrium period then is the following:

$$P_{eq.disc} = 2^{15/14} \pi k_t^{1/2} \epsilon^{-1/4} \mu^{6/7} \dot{M}^{-3/7} (GM)^{-5/7} = 5.47 \mu_{30}^{6/7} \dot{M}_{16}^{-3/7} \text{ s}. \quad (8)$$

For wind accretion:

$$P_{eq.wind} = \sqrt{\frac{k_t \pi}{2\eta}} P_{orb}^{1/2} v^2 (GM)^{-3/2} \dot{M}^{-1/2} \mu = 47.29 (P_{orb}/10 \text{ days})^{1/2} \mu_{30} v_8^2 \dot{M}_{16}^{-1/2} \text{s}. \quad (9)$$

Here \dot{M}_{16} is the accretion rate normalized to a typical value 10^{16}g s^{-1} , μ_{30} is the magnetic moment normalized to a typical value 10^{30}G cm^3 , and $v_8 = v/10^8 \text{cm s}^{-1}$ is the velocity of the accreting matter.

Assuming that the spin period of a NS is equal to its equilibrium period, the magnetic field B for disc accretion can be estimated as follows:

$$B = 2^{-1/4} \pi^{-7/6} k_t^{-7/12} \epsilon^{7/24} P^{7/6} \dot{M}^{1/2} (GM)^{5/6} R^{-3}. \quad (10)$$

For wind accretion:

$$B = 2 \sqrt{\frac{2\eta}{k_t \pi}} P_{orb}^{-1/2} v^{-2} (GM)^{3/2} \dot{M}^{1/2} P R^{-3}. \quad (11)$$

3.2. Estimate based on the maximum spin-down rate

This method is described, for instance, in Lipunov (1992).

Observations show that NSs in binaries exhibit episodes of deceleration and acceleration. At the moment of the maximum spin-down the decelerating torque is much larger than the accelerating one. In this case we can neglect the first term in eq. (7) and obtain the following:

$$\frac{dI\omega}{dt} = -k_t \frac{\mu^2}{R_{co}^3}. \quad (12)$$

Using the observed values of the maximum spin-down rate the magnetic field of a NS can be estimated as follows:

$$B = \frac{2}{R^3} \left(\frac{I \dot{P} GM}{2\pi k_t} \right)^{1/2}. \quad (13)$$

This estimate should be normally considered as a lower limit, since we cannot be sure that no accelerating torque exists at that moment.

The data to distinguish episodes of the maximum spin-down and to determine the value of \dot{P} is taken from graphs in Galache et al. (2008). As sources are transient and accretion occurs mainly close to the periastron passage, we use only data points from the same episode of accretion to determine the maximum spin-down rate.

3.3. Estimate based on the maximum spin-up rate

The description of this approach also can be found in Lipunov (1992).

At the moment of the maximum spin-up the accelerating torque is much larger than the decelerating one. In this case we can neglect the second term in eq. (7) and obtain the following:

$$\frac{dI\omega}{dt} = \dot{M}(GM\epsilon R_A)^{1/2}. \quad (14)$$

This equation is written for the case of disc accretion. Using the observed values of the maximum spin-up rate, the magnetic field of NS can be estimated as follows:

$$B = \frac{2^4 \pi^{7/2}}{\epsilon^{7/4}} \frac{(I\dot{P})^{7/2}}{R^3 P^7 \dot{M}^3 (GM)^{3/2}}. \quad (15)$$

This estimate should be normally considered as a lower limit to the value of the magnetic field, since we cannot be sure that no decelerating torque exists at that moment.

We use graphs in Galache et al. (2008) to find episodes of the maximum spin-up and to determine the value of \dot{P} as described in the previous subsection.

3.4. Onset of accretion and the condition $R_A = R_{co}$

In our work we consider only Be/X-ray binaries. Many systems of this type have large eccentricities. During its orbital motion a NS can switch from the propeller to the accretor phase. At this moment the condition $R_A = R_{co}$ is roughly satisfied:

$$\left(\frac{\mu^2}{2\dot{M}\sqrt{GM}} \right)^{2/7} = \left(\frac{GMP^2}{4\pi^2} \right)^{1/3}. \quad (16)$$

We assume that at this moment pulsations start being registered. Using spin period and luminosity we can estimate the magnetic field using the eq. (16) as follows:

$$B = 2^{-4/7} \pi^{-7/6} R^{-3} (\dot{M})^{1/2} (GM)^{5/6} P^{7/6}. \quad (17)$$

3.5. The model by Illarionov and Kompaneets

Above we described the well-known approaches developed by different authors in 70s-80s (see a review in Lipunov (1992)). Now we come to more sophisticated models, starting with the model proposed by Illarionov and Kompaneets (1990).

This is a model with a more efficient spin-down mechanism of an accreting NS. The spin-down is a result of an efficient angular momentum transfer from the rotating magnetosphere of an accreting object to the outflowing stream of magnetized matter. The outflow is formed within a limited solid angle, and the outflow mass rate is less than the accretion rate. Frozen magnetic fields in the outflow may provide additional angular momentum losses.

We assume, that at the moment of the maximum spin-down the decelerating torque is much larger than the accelerating one. This decelerating torque is estimated according to the model by Illarionov and Kompaneets.

The angular momentum losses in a solid angle χ of an outflow can be written as follows (Illarionov and Kompaneets, 1990):

$$\frac{dI\omega}{dt} = -k\frac{\chi}{2\pi}\dot{M}\omega R_A. \quad (18)$$

We use this approach to obtain the decelerating torque in a small solid angle $\chi \sim 1$. For the rest of the NS magnetosphere we assume that the spin-down mechanism described above (eq. 12) is valid. Then the equation for the spin evolution of a NS can be written in the following way, neglecting the accelerating moment:

$$\frac{dI\omega}{dt} = -k\frac{\chi}{2\pi}\dot{M}\omega R_A^2 - k_t\frac{(4\pi - \chi)\mu^2}{4\pi R_{co}^3}. \quad (19)$$

To our knowledge, there is no analytical solution for this equation for magnetic field strength. Therefore we solve it numerically using bisection method. For numerical estimates below we use the following parameter values: $\chi = 1$, $k = 2/3$, and $k_t = 1/3$. We estimate a NS magnetic field from this equation using measured P and \dot{P} which are taken from graphs in Galache et al. (2008).

3.6. The model by Bisnovatyi-Kogan

In the model by Bisnovatyi-Kogan (1991) the author proposed to evaluate spin periods of NSs as: $P = \sqrt{P_1 P_2}$. Here P_1 is the equilibrium period of a

NS. The decelerating torque calculated according to the model by Illarionov and Kompaneets (eq. 18) is compensated by an accelerating torque (see eq. 5):

$$k \frac{\pi R_G^2}{P_{orb}} = \frac{\pi^2 R_A^3}{P_1^2} \sqrt{\frac{R_A}{2GM}} \quad (20)$$

Here we use the Alfven radius in the form $R_A = (B^2 R^6 / (8\dot{M}\sqrt{GM}))^{2/7}$, where B is the field at the magnetic pole. The numerical coefficient k is assumed to be 2/3.

The equilibrium period in this case can be calculated as follows:

$$P_1 = \frac{\sqrt{\pi} P_{orb}^{1/2} v^2 B R^3}{2^{11/4} \sqrt{k} (\dot{M})^{1/2} (GM)^{3/2}} \quad (21)$$

Another characteristic period, P_2 , is estimated in assumption that the angular velocity of the NS is equal to the angular velocity of the infalling matter on the distance of half Alfven radius:

$$\frac{2\pi}{P_2} = \frac{8\pi R_G^2}{P_{orb} R_A^2} \quad (22)$$

This equation differs from the equation given in (Bisnovatyi-Kogan, 1991) by a factor of two.

From equation (22) the period P_2 can be estimated as:

$$P_2 = \frac{v^4 P_{orb} B^{8/7} R^{24/7}}{8^{4/7} 16 \dot{M}^{4/7} (GM)^{16/7}}. \quad (23)$$

Therefore, the spin period of a NS can be calculated as follows:

$$P = \sqrt{P_1 P_2} = 0.37 \frac{v^3 P_{orb}^{3/4} B^{15/14} R^{45/14}}{\dot{M}^{15/28} (GM)^{53/28}}. \quad (24)$$

Using relation (24) we can estimate the magnetic field as follows:

$$B = 2.95 \frac{P^{14/15} \dot{M}^{1/2} (GM)^{53/30}}{v^{14/5} P_{orb}^{7/10} R^3}. \quad (25)$$

3.7. Hybrid model

Recently, a new detailed model for the case of quasi-spherical accretion was developed by Shakura et al. (2011). In this model a settling subsonic accretion proceeds through a hot shell formed around a NS magnetosphere. The turbulent stresses are capable of carrying the angular momentum outwards through the shell.

In this way it is possible to estimate the magnetic field of a NS as follows:

$$B_{12} = 0.24 \left(\frac{\delta^2 \varpi \xi^{-12/33}}{1 - z/Z} \right)^{11/12} \left(\frac{P/100\text{s}}{P_{orb}/10\text{days}} \right)^{11/12} \dot{M}_{16}^{1/3} v_8^{-11/3}. \quad (26)$$

Here we assume that the spin period is equal to the equilibrium value and $B_{12} = (B/10^{12})$ G. The expression in the brackets $(\delta^2 \varpi \xi^{-12/33})/(1 - z/Z)$ is approximately equal to 1 (Shakura et al., 2011). $\delta, \varpi, \xi, z,$ and Z – are numerical coefficients.

The model developed by Shakura et al. (2011) is applicable to long period NSs with quasi-spherical accretion. Accretion in Be/X-ray binaries can proceed with or without formation of an accretion disc around a compact object. It is important to distinguish objects where an accretion disc can be formed. There is a well-known condition for accretion disc formation (see, for instance, Illarionov and Sunyaev (1975)):

$$\eta \Omega R_G^2 > (GMR_A)^{1/2}. \quad (27)$$

The values of numerical coefficient η depend on the structure of stellar wind, presence of inhomogeneities and other properties of accreting matter. For large values of $\eta \sim 1$ an accretion disc is formed for all of the systems under discussion. Davies and Pringle (1980) showed that the coefficient can be much smaller than 1. In this case an accretion disc may fail to form for systems with large values of spin period (Davies and Pringle, 1980). We take into account this condition for the model by Shakura et al. We apply this model only to objects with $P > 50$ s. For short-period objects ($P < 50$ s) we make calculations with the hypothesis of the equilibrium period using standard formulae for disc accretion. So, we call this model "the hybrid".

4. Observational data

For our estimates we use data (Galache et al., 2008) on 40 Be/X-ray binaries in the SMC observed by the RXTE satellite. These data include: the

spin period and count rate (in counts $\text{PCU}^{-1}\text{s}^{-1}$) for the pulsating component of emission. We convert counts to flux using WebPIMMS². Besides the standard RXTE PCA parameters we need to specify the Galactic hydrogen column density (n_H) towards the SMC and spectral parameters.

For the Galactic hydrogen column density in the direction of the SMC we take the value $n_H = 4 \cdot 10^{22} \text{cm}^{-2}$ (Kuulkers et al., 2007). Our results are not very sensitive to this parameter. Even a significant variation of n_H by a factor of a few results in the magnetic field variation on the level of a few percent.

We assume that spectra can be well approximated by a single power-law. So, the only spectral parameter is the photon index. The photon index of all sources is taken to be equal to 1 (Lipunov, 1992). The magnetic field estimates show only modest sensitivity to this parameter. When we change a photon index by a factor of 1.5, the magnetic field changes by $\sim 10\%$.

For our magnetic field estimates we need to know the value of the accretion rate, \dot{M} . We derive it from the X-ray flux value. Formally, we have to use the bolometric flux, however we use a simplified approach. From the measured count rate we derive the flux in some output energy range using WebPIMMS, assuming a single power-law spectrum. To estimate the output energy range we consider the data for different Be/X-ray systems in the Galaxy from the paper (Lutovinov and Tsygankov, 2008). In this work it is shown that most of the objects have power-law spectra up to 25 keV, and we accept this value for our study. The lower limit – 3 keV – for the output energy is taken from (Galache et al., 2008). So, we have the output energy range 3-25 keV to estimate the luminosity used in \dot{M} calculations.

In (Galache et al., 2008) only the data on pulsed flux are given. For our estimates we need to make assumptions about the total flux, as finally we need to derive the value of the mass accretion rate. Obviously, the ratio between pulsed and total fluxes may be different for different sources. However, after a statistical study we decide to use a single value for the whole set of sources, as no details are available for most of the objects in the sample. We assume that the total flux is 5 times larger than the pulsed flux (Lutovinov, private communication).

²<http://heasarc.gsfc.nasa.gov/Tools/w3pimms.html>

5. Results

Our main results consist of estimates of NSs magnetic field in Be/X-ray binaries obtained by several different methods described in Sec. 3. They are presented in Figs. 2 and 3. Estimates for different models are shown with different symbols. In Fig. 2 estimates of magnetic field with the assumption of the equilibrium period hypothesis are plotted as filled circles, and as open circles in cases of wind and disc accretion, respectively. Estimates for the hypothesis of the maximum spin-down and spin-up are drawn as down triangles and up triangles, correspondingly. In Fig. 3 with filled triangles we show estimates of magnetic fields with the assumption of the onset of pulsations when $R_A = R_{co}$, and for the model by Illarionov and Kompaneets — as diamonds. Finally, for the model by Bisnovatyi-Kogan and the hybrid model our results are given as crosses and asterisks correspondingly.

It is expected that the spin periods are on average larger for NSs with larger magnetic fields. This is due to the fact that for a given spin period for larger magnetic field the decelerating torque is much larger, see eq. (7), but the accelerating one remains unchanged (for quasi-spherical accretion), or just slightly increases (if an accretion disc is formed). So, the equilibrium is reached at longer spin periods for larger fields. The accelerating moment linearly depends on the accretion rate; in the case of wind accretion without a disc it also depends on the properties of the binary. This normally should result in a scatter in the relation between spin periods and magnetic fields.

In Figs. 2 and 3 we see that for some models the correlation between spin period and magnetic field of NS is very tight. This can be a result of a selection effect. In our case pulsations are registered only above some flux value. All sources are nearly at the same distance. Then we immediately obtain that in our approach there is a critical value of \dot{M} , below which pulsations are undetectable. This effect is especially important for the model of equilibrium period, for the hybrid model, and for the onset of accretion when $R_A = R_{co}$. Therefore, this effect makes the correlation $B - P$ very tight reducing the scatter.

There is a well-known problem that for long-period objects traditional methods (equilibrium period, $R_A = R_{co}$, and the maximum spin-down, see Lipunov (1992)) often produce too large field value estimates. This is clearly visible in Fig.2. On the other hand, the model of the maximum spin-up shows more realistic results. Still, this method strongly depends on measured parameters. Using the data given in Galache et al. (2008) we cannot

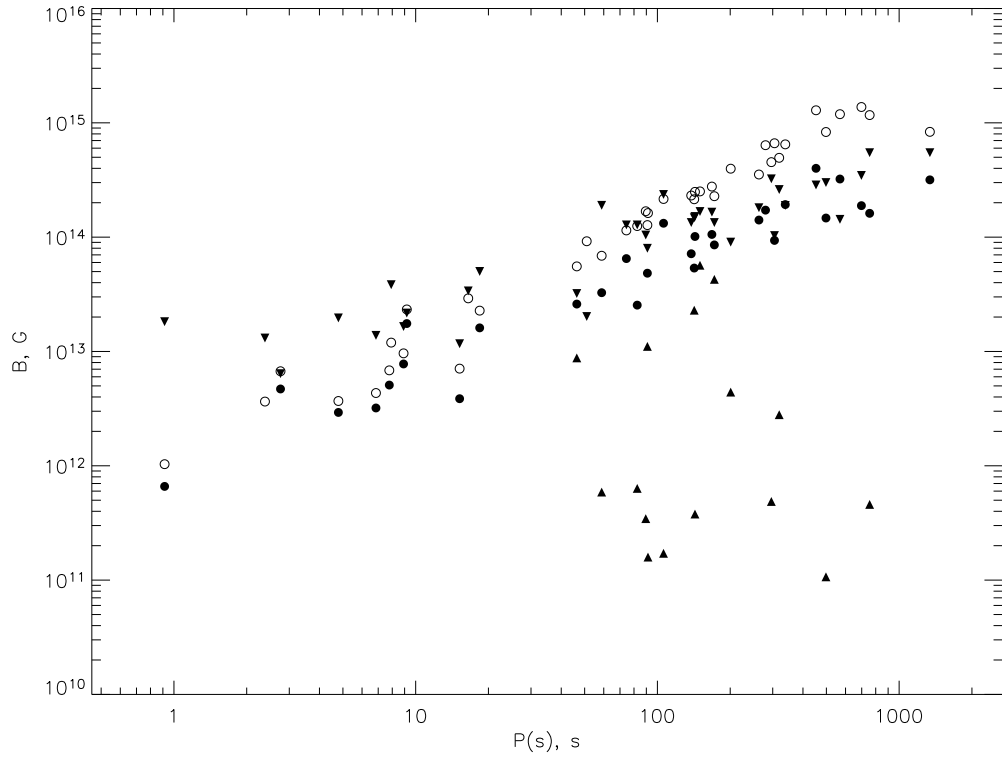


Figure 2: Magnetic field values estimated using different methods: filled circles – the equilibrium period hypothesis in the case of wind accretion, open circles – the equilibrium period hypothesis in the case of disc accretion, down triangles – the maximum spin-down, up triangles – the maximum spin-up.

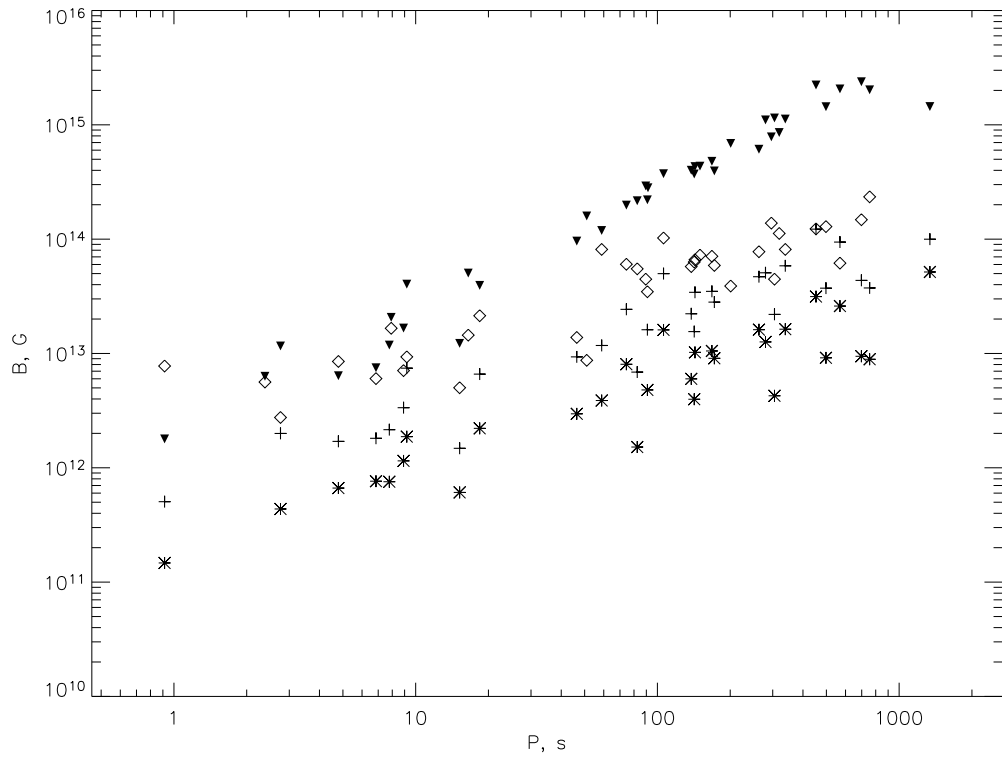


Figure 3: Magnetic field values estimated using different methods (continued): filled triangles – onset of pulsations when $R_A = R_{co}$, asterisks – the hybrid model, diamonds – the model by Illarionov and Kompaneets, and crosses – the model by Bisnovatyi-Kogan.

measure period variations and corresponding time intervals with high precision. The spin periods are presented in the plots with large error bars, and time intervals corresponding to episodes of the maximum spin-up are very short. Therefore the values of \dot{P} are obtained with significant uncertainties, so estimates obtained with this method are not very certain. However, we present results based on the maximum spin-up for long-period sources for which estimates seem to be reliable.

Estimates based on the model by Bisnovatyi-Kogan are more reliable than those based on the maximum spin-up, and do not contain very high values $\gtrsim 10^{14}$ G. Therefore, there are many NSs with $B > 3 \times 10^{13}$ G in contradiction with theoretical expectations.

Finally, the hybrid model is able to reproduce most of the predicted deficit of long-period high magnetic field objects. Thus, we consider this model to be the best among studied and discuss results based on it in the next section in more details.

6. Discussion

In Fig. 4 we show magnetic field distributions. Here the theoretical distribution for the initial polar magnetic field B_0 is generated randomly for 10^5 NSs from a log-normal distribution with the mean value $\langle \log B_0/[G] \rangle = 13.25$ and standard deviation $\sigma_{\log B_0} = 0.6$ (Popov et al., 2010). Note, that formally this initial field distribution is not absolutely self-consistent with our model of field decay, because we use parameters slightly different from those used in numerical calculations by (Popov et al., 2010). However, this imperfection cannot significantly influence our conclusions, because the main assumption is related to the asymptotic field value.

The evolved fields are calculated according to eq. (3) using the values: $\tau_{Hall} = 10^4(B_0/10^{15}\text{G})^{-1}$ yrs and $\tau_{Ohm} = 10^6$ yrs. The NS ages are chosen uniformly in the interval $[0, t_{max}]$, where $t_{max} = 10^7$ yrs is the maximum life time of Be/X-ray binaries. Magnetic field estimates obtained in this paper are shown in four different panels in Fig. 4. In the panel A with a solid line we show the magnetic field distribution based on the assumption of the onset of pulsations when $R_A = R_{co}$. The magnetic field distribution according to the model by Bisnovatyi-Kogan is plotted in the panel B. Distributions for the models by Illarionov, Kompaneets and the hybrid model are shown in the panels C and D, correspondingly. Theoretical models for the initial and the

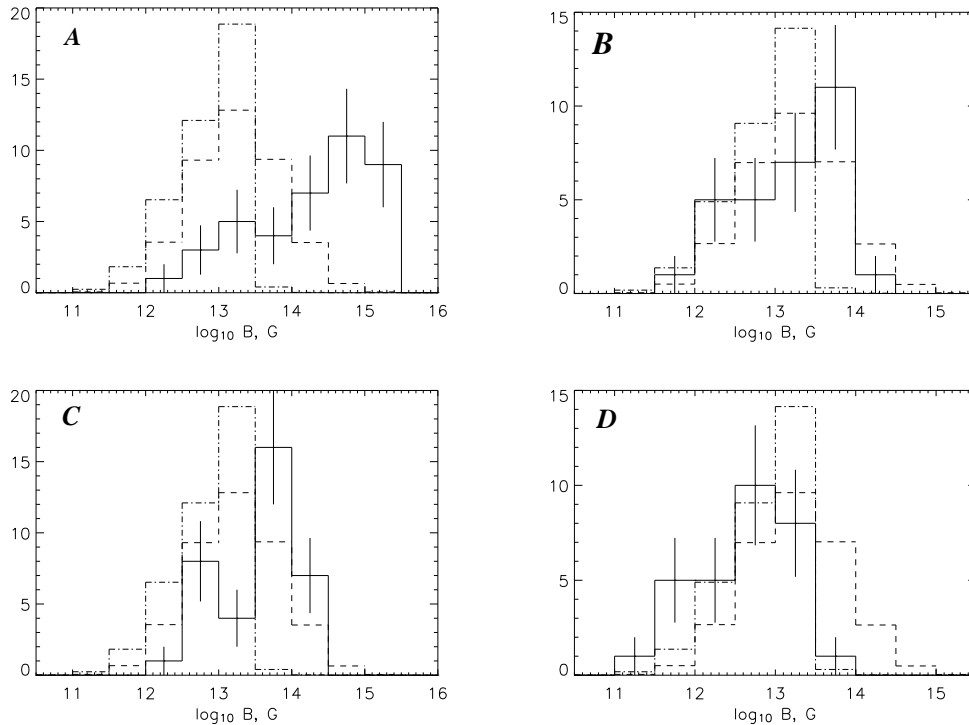


Figure 4: Magnetic field distributions for different models (solid lines). Panel A – onset of pulsations when $R_A = R_{co}$. Panel B – the model by Bisnovatyi-Kogan. Panel C – the model by Illarionov and Kompaneets. Panel D – the hybrid model. Theoretical models for the initial and evolved magnetic fields are shown in all the four panels by dashed and dash-dotted lines, respectively. All distributions are normalized to the total number of observed objects. Error bars are given according to the Poissonian values.

evolved magnetic fields are shown in all four panels by dotted and dot-dashed lines, correspondingly.

To compare the theoretical predictions with results based on the hybrid model we use the Kolmogorov-Smirnov test. According to this test, the hypothesis of the same distribution of the theoretical and estimated values cannot be rejected at 80% significance level. However, there is a small number of objects for the hybrid model distribution in the bin $10^{13} < B < 10^{13.5}$ G (Fig. 4D). Discrepancies can be related to uncertainty in evolution of the magnetic field for $t > 10^6$ yrs. Probably, the magnetic field decay continues but more slowly than before. Likewise, different highly magnetized objects can evolve to different values of the asymptotic magnetic field (see Sec. 2).

In this study we assumed that NSs in binaries have the same initial magnetic distribution as isolated compact objects. This is not so obvious in the case of magnetars, as in the standard scenario their magnetic fields are generated via the dynamo mechanism (Duncan and Thompson, 1992). The dynamo mechanism is effective in the case of very rapid rotation of a protoNS. Isolated massive stars hardly can have rapidly rotating cores. Rapid rotation can be reached in close binary systems due to accretion or/and tidal synchronization. On the other hand, all known magnetars are isolated objects, and authors studied evolutionary channels in binary systems which result in formation of isolated compact objects with rapid initial rotation (Bogomazov and Popov, 2009; Popov and Prokhorov, 2006). In these models objects with extremely large field tend to form after a binary is destroyed to explain that all known magnetars are isolated.

To test the possibility of absence of extreme magnetars in binary systems for the case of the hybrid model (which is the most successful in explaining the properties of the population under study), we plot an additional histogram (Fig. 5) for a modified initial magnetic field distribution: no NSs with $B_0 > 10^{14}$ G are formed. As we see, estimates made on the basis of observational data are even in better agreement with the prediction for the evolved field in the model by Pons et al. (2009) with the cutoff at $B_0 = 10^{14}$ G, as the discrepancy in the bin $10^{13} < B < 10^{13.5}$ G is decreased. However, we note that our calculations are based on an approximation to the actual detailed model by Pons et al. (2009), and for the specific choice of parameters, which can vary ($\tau_{Hall}, \tau_{Ohm}, B_{min}$). We do not overestimate the accuracy of our results, and so do not make further speculations.

An additional consistency check for magnetic field estimates can be made using the Corbet diagram (Corbet, 1984). We apply this test to the hybrid model. This diagram relates spin periods and orbital periods of NSs. We simulate this distribution. Orbital periods of NSs are chosen uniformly in the interval [10, 1000] days. Using an orbital period and evolved magnetic field we can estimate the spin period of a NS. We calculate the evolved magnetic field as discussed above. These values of spin and orbital periods are plotted in Fig. 6 as dots. We plot the observational data (Reig, 2011) as diamonds in this figure. One can see good agreement between theoretical and observational data. According to the non-parametric Kolmogorov-Smirnov test, the hypothesis that both subsets arise from the same distribution cannot be rejected at 77% significance level.

The methods that we use to estimate magnetic fields have limitations,

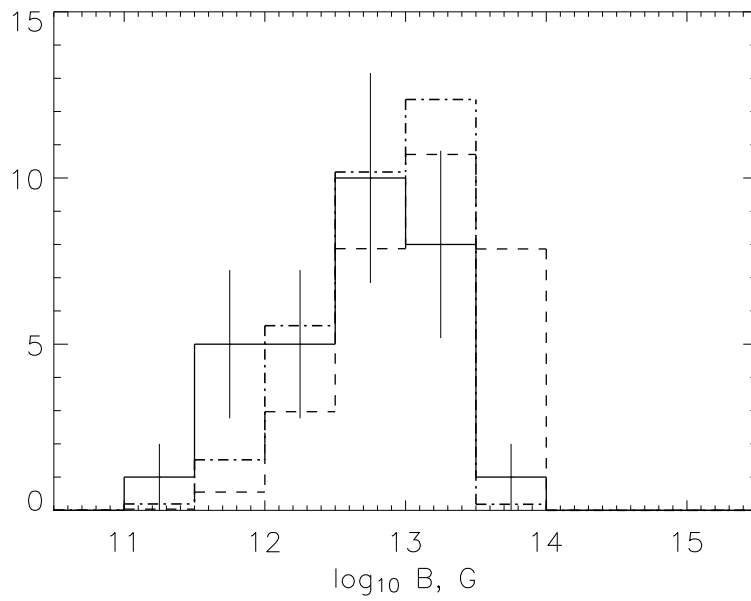


Figure 5: Magnetic field distributions. The distribution based on observational data after application of the hybrid model is shown with a solid line. Poissonian error bars are indicated. Results for the theoretical model for evolved magnetic fields is shown with a dash-dotted line. Finally, a modification of the theoretical model for which a cut-off at 10^{14} G for initial fields was used is shown with a dashed histogram. All distributions are normalized to the total number of observed objects.

especially the most simple ones. For instance, the hypothesis of the equilibrium period may not be valid for some systems. In our estimates we use \dot{M} obtained for the moment when pulsations are detected for the first time. But for NSs in systems with high eccentricity which spend much time at the propeller stage, it can take some time to reach the equilibrium. So, their observed periods are larger than the equilibrium value. This results in underestimating of the magnetic field.

Likewise, we should consider that both disc and wind accretion estimates (see, Fig. 2) cannot be correct at the same time because just one regime is realized in any given source. On average, estimates for disc accretion are more realistic for shorter spin periods. Still, we think that estimates based on old models are not realistic in general, as they produce too large field values for long period sources.

In the model by Shakura et al. (2011) there is a critical value of \dot{M} . For accretion rates above this \dot{M}_{cr} an envelope around a compact object can cool rapidly. This results in an enhanced accretion rate, and no equilibrium is possible in this regime. This critical value depends on several parameters and can be different in different systems, but roughly $\dot{M}_{cr} \lesssim 10^{17}$ g/s for magnetic fields $\gtrsim 10^{13}$ G. Marginally, this condition is fulfilled for our systems. We can slightly overestimate the accretion rate, however, if the model by Shakura et al. (2011) is applicable, then the magnetic field estimate depends on the accretion rate only mildly.

It is instructive to compare the results of indirect magnetic field estimates with direct magnetic field measurements through cyclotron lines, as it was made for the long-period object GX 301-2. For this object, magnetic field strength is estimated by La Barbera et al. (2005) as $\sim 5 \times 10^{12}$ G. This value is consistent with the magnetic field estimate made by Shakura et al. (2011) using their model. On the other hand, the classical models used by Doroshenko et al. (2010) provide the magnetic field estimate nearly two orders of magnitude larger than it is given by the cyclotron line measurements. However, the cyclotron line can be formed high above the NS surface that allows the measured magnetic field strength to be considerably weaker than that on the surface (Doroshenko et al., 2010).

Finally, we comment on a possible evolution of the angle between spin and magnetic axis. For radio pulsars it is possible to describe the angular momentum evolution using the magneto-dipole formula (Pacini, 1967):

$$\frac{dI\omega}{dt} = -\frac{1}{6} \frac{B^2 \omega^3 R^6}{c^3} \sin^2 \beta, \quad (28)$$

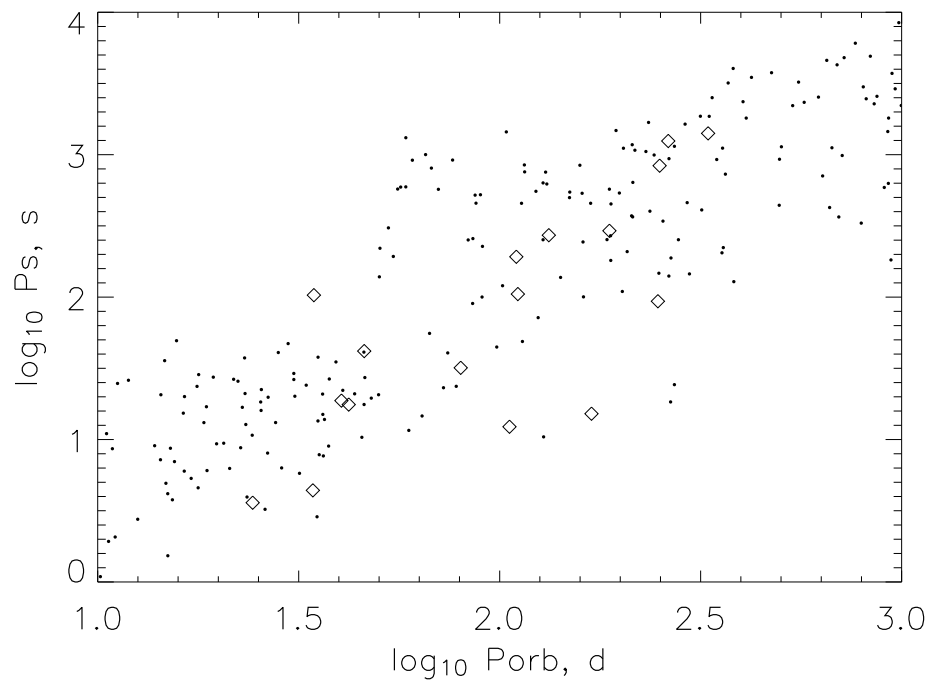


Figure 6: Corbet diagram for the observed data (open diamonds) and for the hybrid model (dots).

Here β is the angle between spin and magnetic axis. From this formula one can estimate the effective magnetic field $B_{eff} = B\sin\beta$. So, the effect of the variation of the effective magnetic field can be related not only to the magnetic field decay, but also to evolution of the angle between magnetic and spin axis. Therefore, it is difficult to distinguish between these effects. However, there are different methods to estimate magnetic field of magnetars and to demonstrate that this is really the field decay, not the variation of the angle β . Note, that our methods are only weakly sensitive to the angle between spin and magnetic axis, and we estimate the absolute value of magnetic field. Still, using Be/X-ray systems we can try to study evolution of the angle between these axis. According to two most popular models (magneto-dipole and current losses), the angle evolves very fast on the time scale of spin period evolution. The angle β evolves to the value $\beta = 0^\circ$ in the magneto-dipole model and to the value $\beta = 90^\circ$ in the current losses model (Gurevich et al., 1993). But this effect is not observed for PSRs. It is possible to use Be/X-ray binaries to study evolution of the angle on the time scale up to 10^7 yrs jointly with the magnetic field decay. We plan to use this approach in future studies.

7. Summary

In our work we used different models to estimate magnetic fields of NSs in Be/X-ray binaries in the SMC. Most of them are shown to overestimate the magnetic field, but the hybrid model based on the approach by Shakura et al. (2011) gives good agreement with the prediction of the theoretical model of magnetic field decay on a time scale up to $\sim 10^7$ yrs.

Acknowledgements

We thank N.I. Shakura and K.A. Postnov for the opportunity to use their model before publication, and for consultations. We acknowledge A.A. Lutovinov and J.A. Pons for interesting discussions. We thank P.K. Abolmasov and E.A. Vasiliev for useful remarks. Also we are grateful to the anonymous referees for useful comments. Sergei Popov thanks University of Padova for support and hospitality during his visit. This work was supported by the Russian Foundation for Basic Research grants 10-02-00599, 12-02-00186 and by the Federal program for research staff (02.740.11.0575).

References

- Aguilera, D.N., Pons, J.A., Miralles, J.A., 2008. The Impact of Magnetic Field on the Thermal Evolution of Neutron Stars. *ApJL* 673, L167–L170. [arXiv:0712.1353](#).
- Bhattacharyya, S., 2009. X-ray views of neutron star low-mass X-ray binaries. *Current Science* 97, 804–820. [arXiv:1002.4480](#).
- Bisnovaty-Kogan, G.S., 1991. Rotational equilibrium of long-periodic X-ray pulsars. *A&A* 245, 528–530.
- Bogomazov, A.I., Popov, S.B., 2009. Magnetars, gamma-ray bursts, and very close binaries. *Astronomy Reports* 53, 325–333. [arXiv:0905.3238](#).
- Corbet, R.H.D., 1984. Be/neutron star binaries - A relationship between orbital period and neutron star spin period. *A&A* 141, 91–93.
- Davies, R.E., Pringle, J.E., 1980. On accretion from an inhomogeneous medium. *MNRAS* 191, 599–604.
- de Luca, A., 2008. Central Compact Objects in Supernova Remnants, in: C. Bassa, Z. Wang, A. Cumming, & V. M. Kaspi (Ed.), *40 Years of Pulsars: Millisecond Pulsars, Magnetars and More*, pp. 311–319. [arXiv:0712.2209](#).
- Doroshenko, V., Santangelo, A., Suleimanov, V., Kreykenbohm, I., Staubert, R., Ferrigno, C., Klochkov, D., 2010. Is there a highly magnetized neutron star in GX 301-2? *A&A* 515, A10. [0907.3844](#).
- Duncan, R.C., Thompson, C., 1992. Formation of very strongly magnetized neutron stars - Implications for gamma-ray bursts. *ApJL* 392, L9–L13.
- Galache, J.L., Corbet, R.H.D., Coe, M.J., Laycock, S., Schurch, M.P.E., Markwardt, C., Marshall, F.E., Lochner, J., 2008. A Long Look at the Be/X-Ray Binaries of the Small Magellanic Cloud. *ApJ Supp.* 177, 189–215. [arXiv:0802.2118](#).
- Goldreich, P., Reisenegger, A., 1992. Magnetic field decay in isolated neutron stars. *ApJ* 395, 250–258.

- Gurevich, A., Beskin, V., Istomin, Y., 1993. *Physics of the Pulsar Magnetosphere*, pp. 432. ISBN 0521417465. Cambridge, UK: Cambridge University Press, August 1993.
- Haberl, F., 2007. The magnificent seven: magnetic fields and surface temperature distributions. *Astrophys. & Space Sciences* 308, 181–190. [arXiv:0609066](#).
- Illarionov, A.F., Kompaneets, D.A., 1990. A Spin-Down Mechanism for Accreting Neutron Stars. *MNRAS* 247, 219.
- Illarionov, A.F., Sunyaev, R.A., 1975. Why the Number of Galactic X-ray Stars Is so Small? *A&A* 39, 185.
- Kaplan, D.L., 2008. Nearby, Thermally Emitting Neutron Stars, in: C. Bassa, Z. Wang, A. Cumming, & V. M. Kaspi (Ed.), *40 Years of Pulsars: Millisecond Pulsars, Magnetars and More*, pp. 331–339.
- Keane, E.F., 2010. Transient Radio Neutron Stars [arXiv:1008.3693](#).
- Kuulkers, E., Shaw, S.E., Paizis, A., Chenevez, J., Brandt, S., Courvoisier, T., Domingo, A., Ebisawa, K., Kretschmar, P., Markwardt, C.B., Mowlavi, N., Oosterbroek, T., Orr, A., Rísquez, D., Sanchez-Fernandez, C., Wijmands, R., 2007. The INTEGRAL Galactic bulge monitoring program: the first 1.5 years. *A&A* 466, 595–618. [arXiv:0701244](#).
- La Barbera, A., Segreto, A., Santangelo, A., Kreykenbohm, I., Orlandini, M., 2005. A study of an orbital cycle of GX 301-2 observed by BeppoSAX. *A&A* 438, 617–632.
- Lipunov, V.M., 1992. *Astrophysics of Neutron Stars, XIII*, 322 pp. 108 figs. Springer-Verlag Berlin Heidelberg New York.
- Liu, Q.Z., van Paradijs, J., van den Heuvel, E.P.J., 2006. Catalogue of high-mass X-ray binaries in the Galaxy (4th edition). *A&A* 455, 1165–1168. [arXiv:0707.0549](#).
- Lutovinov, A., Tsygankov, S., 2008. X-ray pulsars through the eyes of INTEGRAL, in: M. Axelsson (Ed.), *American Institute of Physics Conference Series*, pp. 191–202. [arXiv:0808.2034](#).

- Manchester, R.N., Hobbs, G.B., Teoh, A., Hobbs, M., 2005. The Australia Telescope National Facility Pulsar Catalogue. *AJ* 129, 1993–2006. [arXiv:0412641](#).
- Mereghetti, S., 2008. The strongest cosmic magnets: soft gamma-ray repeaters and anomalous X-ray pulsars. *A&ARv* 15, 225–287. [arXiv:0804.0250](#).
- Negueruela, I., 2010. Stellar Wind Accretion in High-Mass X-Ray Binaries, in: J. Martí, P. L. Luque-Escamilla, & J. A. Combi (Ed.), *High Energy Phenomena in Massive Stars*, p. 57. [arXiv:0907.2883](#).
- Pacini, F., 1967. Energy Emission from a Neutron Star. *Nature* 216, 567–568.
- Pavlov, G.G., Sanwal, D., Teter, M.A., 2004. Central Compact Objects in Supernova Remnants, in: F. Camilo & B. M. Gaensler (Ed.), *Young Neutron Stars and Their Environments*, p. 239. [arXiv:0311526](#).
- Pons, J.A., Geppert, U., 2007. Magnetic field dissipation in neutron star crusts: from magnetars to isolated neutron stars. *A&A* 470, 303–315. [arXiv:0703267](#).
- Pons, J.A., Miralles, J.A., Geppert, U., 2009. Magneto-thermal evolution of neutron stars. *A&A* 496, 207–216. [arXiv:0812.3018](#).
- Popov, S.B., Pons, J.A., Miralles, J.A., Boldin, P.A., Posselt, B., 2010. Population synthesis studies of isolated neutron stars with magnetic field decay. *MNRAS* 401, 2675–2686. [arXiv:0910.2190](#).
- Popov, S.B., Prokhorov, M.E., 2006. Progenitors with enhanced rotation and the origin of magnetars. *MNRAS* 367, 732–736. [arXiv:0505406](#).
- Postnov, K.A., Yungelson, L.R., 2006. The Evolution of Compact Binary Star Systems. *Living Reviews in Relativity* 9, 6. [arXiv:0701059](#).
- Raguzova, N.V., Lipunov, V.M., 1998. High-eccentric X-ray binaries: evolution, wind rose effect, accretor-propeller luminosity gap. *A&A* 340, 85–102.
- Raguzova, N.V., Popov, S.B., 2005. Be X-ray binaries and candidates. *Astronomical and Astrophysical Transactions* 24, 151–185. [arXiv:0505275](#).

- Rea, N., Esposito, P., 2011. Magnetar outbursts: an observational review, in: D. F. Torres & N. Rea (Ed.), High-Energy Emission from Pulsars and their Systems, p. 247. [1101.4472](#).
- Reig, P., 2011. Be/X-ray binaries. *Ap&SS* 332, 1–29. [arXiv:1101.5036](#).
- Shakura, N., Postnov, K., Kochetkova, A., Hjalmarsdotter, L., 2011. Theory of quasi-spherical accretion in X-ray pulsars. accepted for publication in *MNRAS* [arXiv:1110.3701](#).